American Society of
Mechanical Engineers

ASME Accepted Manuscript Repository

Institutional Repository Cover Sheet

Cranfield Collection of E-Research - CERES

First Last

ASME Paper Title: Impact of adverse environmental conditions on rotorcraft operational performance and pollutant emissions

Authors: Jesus Ortiz-Carretero, Alejandro Castillo Pardo, Ioannis Goulos and Vassilios Pachidis

ASME Journal Title: Journal of Engineering for Gas Turbines and Power

Volume/Issue ___Vol. 140, Iss. 2_____ Date of Publication (VOR* Online) _23.8.2017_____

ASME Digital Collection URL: http://gasturbinespower.asmedigitalcollection.asme.org/article.aspx?articleid=2652540

DOI: 10.1115/1.4037751

*VOR (version of record)

Journal of Engineering for Gas Turbines and Power, 2017, Volume 140, Issue 2, Article number 021201, October 2017
Paper Number GTP-17-1313. DOI:10.1115/1.4037751

IMPACT OF ADVERSE ENVIRONMENTAL CONDITIONS ON ROTORCRAFT OPERATIONAL PERFORMANCE AND POLLUTANT EMISSIONS

Jesus Ortiz-Carretero[*]
Doctoral Researcher
Propulsion Engineering Centre
Cranfield University
Bedfordshire MK43 0AL, UK
E-mail: j.ortizcarretero@cranfield.ac.uk

Alejandro Castillo Pardo
Doctoral Researcher
Propulsion Engineering Centre
Cranfield University
Bedfordshire MK43 0AL, UK
E-mail: a.castillopardo@cranfield.ac.uk

Ioannis Goulos
Lecturer in Propulsion Integration
Propulsion Engineering Centre
Cranfield University
Bedfordshire MK43 0AL, UK
E-mail: i.goulos@cranfield.ac.uk

Vassilios Pachidis
Professor of Propulsion Integration Engineering
Propulsion Engineering Centre
Cranfield University
Bedfordshire MK43 0AL, UK
E-mail: v.pachidis@cranfield.ac.uk

ABSTRACT

It is anticipated that the contribution of rotorcraft activities to the environmental impact of civil aviation will increase in the future. Due to their versatility and robustness, helicopters are often operated in harsh environments with extreme ambient conditions. These severe conditions, not only affect the performance of the engine, but also the aerodynamics of the rotorcraft. This impact is reflected in the fuel burn and pollutants emitted by the rotorcraft during a mission. The aim of this paper is to introduce an exhaustive methodology to quantify the influence adverse environment conditions have in the mission fuel consumption and the associated emissions of nitrogen oxides (NO_x). An Emergency Medical Service (EMS) and a Search and Rescue (SAR) mission are used as case studies to simulate the effects of extreme temperatures, high altitude, and compressor degradation on a representative Twin-Engine Medium (TEM) weight helicopter, the Sikorsky UH-60A Black Hawk. A simulation tool for helicopter mission performance analysis developed and validated at Cranfield University was employed. This software comprises different modules that enable the analysis of helicopter flight dynamics, powerplant performance and exhaust emissions over a user defined flight path profile. For the validation of the models implemented, extensive comparisons with experimental data are presented throughout for rotorcraft and engine performance as well as NO_x emissions. Reductions as high as 12% and 40% in mission fuel and NO_x emissions, respectively, were

[*] Corresponding author

Published by ASME. This is the Author Accepted Manuscript issued with: Creative Commons Attribution Non-Commercial License (CC:BY 4.0).
The final published version (version of record) is available online at DOI:10.1115/1.4037751. Please refer to any applicable publisher terms of use.

observed for the 'High & Cold' scenario simulated at the SAR role relative to the same mission trajectory under standard conditions.

NOMENCLATURE

Acronyms

AGL	Above Ground Level
AUM	All-Up Mass [kg]
CO_2	Carbon dioxide
DP	Design Point
DZ	Dilution Zone
EI	Emission Index [g/kg fuel]
EMS	Emergency Medical Service
F	Flap vibration mode
FF	Flame Front
HECTOR	Helicopter Omni-disciplinary Research platform
ISA	International Standard Atmosphere
IZ	Intermediate Zone
L	Lag vibration mode
MCP	Maximum Continuous Power
MR	Main Rotor
NO_x	Nitrogen oxides
OD	Off-Design
P	Rotational speed multiple
PR	Pressure Ratio
PZ	Primary Zone
SAR	Search and Rescue
SL	Sea Level
T	Torsion vibration mode
TEM	Twin Engine Medium
TET	Turbine Entry Temperature [K]

TR	Tail Rotor
WGS 84	World Geodetic System dated in 1984

Roman symbols

A	Main rotor disk area [m^2]
$C_p=P_{MR}/\rho A(\Omega R)^3$	Power coefficient [-]
$C_t = T_{MR}/\rho A(\Omega R)^2$	Thrust coefficient [-]
P_{MR}	Main rotor power [W]
R	Main rotor radius [m]
T_{MR}	Main rotor thrust [N]
V	Air speed [m/s]
V_{NOx}	Airspeed for minimum NO_x [m/s]
V_{rg}	Airspeed for maximum range [m/s]
w_f	Powerplant fuel flow [g/s]
w_{NOx}	Powerplant NO_x production [g/s]

Greek symbols

Γ	Mass flow capacity [-]
Δ	Increment [%]
Ω	Main rotor rotational speed [rad/s]
η	Isentropic efficiency [-]
ρ	Air density [kg/m^3]
σ	Main rotor solidity [-]
ω	Blade natural frequency [rad/s]

INTRODUCTION

Background

Rotorcraft are able to undertake missions that are impossible for other aircraft. Thus, they have found a wide range of applications such as medical evacuation, search and rescue and off-shore oil platforms service. These roles often include operation in harsh environments such as deserts, mountain regions and off-shore areas.

The severe conditions helicopters may encounter usually involve atypical atmospheric conditions, which affect significantly the performance of the engine. For instance, the extreme temperatures found in a hot desert have a negative impact on the engine power output and thermal efficiency. To flight at high altitudes also reduces the power generated by the engine, even though its efficiency slightly increases. The atmospheric conditions also affect the performance of the helicopter rotor blades [1]: a reduction in air density, due to either a rise in air temperature or flight altitude, will cause an increase in the power required to hover and fly at low speeds. The opposite effect is seen at high speeds, where the lower air density translates into a reduced power demand as a result of the reduction in fuselage parasitic drag.

Another characteristic of these environments is the presence of particles in the air, such as dirt, salt and sand, which can trigger the deterioration of the engine components due to fouling, erosion and corrosion. Engine deterioration has a detrimental effect on the flow capacity and efficiency of the affected component.

Therefore these demanding environmental conditions are expected to alter the fuel consumption and pollutant emissions of the rotorcraft. The extent by which the environmental footprint of the helicopter is influenced by the ambient conditions is quantified in the present work in order to effectively address in service rotorcraft operation sustainability.

Rotorcraft pollutant emissions

Rotorcraft emissions assessment is an arduous task due to the lack of publicly available engine emissions data and the fact that there is no generally accepted methodology for the helicopter emissions calculation.

In order to fill the existing gap, the Swiss Federal Office of Civil Aviation (FOCA), launched the HELEN (HELicopter Engines) project in January 2008 [2]. As an outcome of this project, several empirical functions were developed from experiments conducted on a wide range of helicopters in order to calculate the fuel flow and the Emission Index (EI) of the most standard pollutants. However, this method has a lack on accuracy of ±15% for fuel prediction and an estimated error of a factor of two or more for emissions calculations. Furthermore, the expressions derived by FOCA are uniquely a function of engine shaft power, which implies that environmental conditions or engine health parameters are not considered.

The aim of this work is to establish a thorough methodology to quantify the effect of environmental conditions on the performance of a helicopter in terms of fuel consumption and NO_x emissions. In order to predict the fuel consumption and pollutant formation, the coupled simulation of the helicopter flight dynamics and gas turbine engine operation is required at different control points during the mission. The in-house TURBOMATCH software developed at Cranfield University [3] is used to simulate the engine performance, whilst the in-house HEPHAESTUS tool [4] is employed to predict the pollutant emission rates. These two computational tools are implemented within a third in-house framework called HECTOR [5] that simulates the rotorcraft flight dynamics. The proposed methodology constitutes a stand-alone platform able to simulate the performance of different helicopters at any user-defined conditions.

The effect of extremely hot temperatures, dust particles ingestion and high altitude are investigated in the present analysis. For this purpose two mission roles are considered which are referred to as Emergency Medical Service (EMS) and Search and Rescue (SAR). Under the EMS mission, the conditions of a hot desert have been reproduced to evaluate the effect of high temperature and engine degradation on the helicopter performance. For the SAR mission, a 'High & Cold' scenario was assumed to assess the effect of low temperature and low air density on the rotorcraft operation. The results obtained at the 'High & Cold' scenario are benchmarked against the results produced when standard environmental conditions are set over the same mission trajectory.

The helicopter platform considered for the analysis is a Twin-Engine Medium (TEM) weight helicopter modeled after the Sikorsky UH-60A Black Hawk powered by two General Electric T700-GE-700 turboshaft engines. This helicopter is a multi-role rotorcraft designed to operate in hostile environments, such as those considered in this work [6]. Extensive data for this particular helicopter is publicly available for validation purposes.

Scope of present work

The numerical framework employed herein to simulate the performance of the helicopter, HECTOR, has been applied in the past to assess fuel consumption and NO_x emissions at rotorcraft mission level [7]. It has been also employed in the optimization of conventional and regenerative powerplants in terms of rotorcraft operational and environmental performance [8,9]. In addition to this work, several studies have been conducted in the optimization of the helicopter flight path and operational procedures for environmental impact mitigation [10,11]. These research activities were completed assuming standard atmospheric conditions and 'clean' powerplants. Thus, no allowance has been made yet for the impact of realistic operational conditions on the final helicopter environmental sustainability.

In order to fill this gap in knowledge, this paper aims to showcase how adverse environmental conditions are expected to impact the rotorcraft performance at aircraft and mission level. To that end, the effects of ambient temperature and flight altitude on forward flight are first analyzed. The effect of helicopter mass is also considered in this part of the analysis. The impact on helicopter power requirement together with the effect these parameters and compressor degradation have on engine performance and NO_x production is assessed. The fluctuation of the airspeeds for maximum range and minimum NO_x formation is also investigated. The performance of the helicopter was then assessed at mission level. In this second part, time-variations of the parameters of interest along the mission, i.e. helicopter total power, engine fuel flow and NO_x production rate, are presented and the total mission results are evaluated.

The present analysis complements the work already developed on the assessment of rotorcraft environmental impact with the inclusion of the environmental conditions as a novelty. The approach offers a first estimation of the impact realistic operational conditions have on the final helicopter performance and its environmental footprint.

MATHEMATICAL MODELING APPROACH

The helicopter flight dynamics are simulated with an in-house rotorcraft comprehensive code named HECTOR (Helicopter Omni-disciplinary Research platform). A detailed description of HECTOR was reported by Goulos [5], and therefore only a brief description of the key models is included in this section. This software permits the comprehensive simulation of three-dimensional helicopter missions employing a cost-effective methodology. HECTOR has been validated and extensively used in previous rotorcraft studies [8,9]. The architecture of the code is shown in Fig. 1.

Aeroelastic rotor model

The aeroelastic rotor model integrated in HECTOR is based on the numerical method described in [5,12] for the simulation of rotor blade elasticity in the time domain. Non-linear inertial terms associated with large blade deflections as well as the helicopter 3-dimensional motion are accounted. The structural formulation of the rotor is model is coupled with the Peters-He finite state induced flow model [13] and the Leishman-Beddoes unsteady nonlinear blade element aerodynamics model [14].

The minimum potential energy approach described in [5] is used to calculate the natural vibration characteristics of the main rotor blades for flap-lag-torsion. Ground effect on the effective main rotor inflow is evaluated through the implicit application of the Cheeseman and Bennet theory [15].

Helicopter flight dynamics model

For the analysis of the helicopter flight dynamics the rotorcraft fuselage is treated as a rigid body with six degrees of freedom, i.e. three translations and three rotations. Look-up tables developed by Padfield [16] are implemented in the code in order to describe the fuselage force and moment coefficients as functions of incidence and sideslip angles. For the tail-rotor performance analysis, steady-state airfoil data together with a first order dynamic inflow formulation [17] are used. Finally, a Newton-Raphson based numerical method is implemented in HECTOR in order to calculate the rotor trim control and fuselage attitude angles for any set of flight conditions.

Flight path definition

The translation of coordinates defined in a global geographical system (latitude and longitude) to the Cartesian system of reference, and vice versa, is required in order to update the position of the rotorcraft throughout the mission. This process is accomplished by the implementation of a set of expressions based on the global representation employed by WGS 84 [18], which is the standard coordinate frame of reference for earth geography definition.

Engine performance simulation (TURBOMATCH)

The engine performance simulation code implemented in HECTOR is the Cranfield University in-house software TURBOMATCH, first developed by MacMillan [3]. This code is a zero-dimensional component-based gas turbine simulation framework, which analyzes the gas path thermodynamics employing discrete component maps. TURBOMATCH has been previously used in several studies to predict the engine performance of different gas turbine engine architectures [19], [20]. This software allows the simulation of Design Point (DP) and Off-Design (OD) performance of any gas turbine configuration, and is able to account for the level of degradation of engine compressor and turbine components.

Engine emissions model (HEPHAESTUS)

The gaseous emissions are predicted with the Cranfield University in-house tool named HEPHAESTUS. A full description of the code theory and validation is provided by Celis [4], and only the main aspects are included herein for completeness. HEPHAESTUS predicts the pollutant emissions based on the ambient conditions, air conditions at the entry of the combustor, fuel properties, combustor geometry and air flow distribution within the combustor liner. The calculation is based on the stirred reactor concept along with a scheme of simplified chemical reactions that estimate the production of different pollutants species during the fuel combustion in conventional combustor chambers.

SIKORSKY UH-60A MODELING AND VALIDATION

The rotorcraft model was developed after the Sikorsky UH-60A Black Hawk helicopter. The UH-60A is a TEM helicopter powered by two General Electric T700-GE-700 turboshaft engines. The main rotorcraft model design parameters are presented in Table 1. The UH-60A Black Hawk has been extensively studied in the past. Numerical and flight test analyses are documented in the literature [21-23], so further description is omitted.

Helicopter flight dynamics

The rotorcraft model implemented in HECTOR has been validated against experimental and flight test data available in the public domain. Figure 2 presents the resonance chart calculated for the UH-60A main rotor. The main rotor blade has been modeled as a spring articulated rotor blade with coincident flap and lag hinges and an elastomeric root in torsion. The natural frequencies and rotor speed have been normalized with the nominal rotor speed (Ω_0). The solid lines represent the calculated natural frequencies, whilst the discrete points correspond to the experimental data. The procedure used to obtain the latter data is described by Hamade *et al* [22]. Overall good agreement between calculated and experimental data is observed for all the natural modes analyzed, with relative errors below 5%. This favorable comparison between calculated and experimental modal characteristics is paramount for the prediction of rotor hub moments and forces, as they determine the rigid and elastic displacements of the blade. An extra natural mode associated with a rigid lead-lag mode is observed which was not reported in the experimental data.

Figure 3 presents the calculated dominant mode shapes for the first nine modes of vibration of the UH-60A main rotor at nominal rotorspeed. Two types of modes are distinguished in this figure: rigid and elastic. Rigid modes of vibration, 1F and 1L, are associated with rigid rotations around the hinges with negligible elastic deformation. Certain elastic curvature is observed next to the hinge due to the presence of discrete flap and lead-lag springs.

Figure 4 presents the variation of the power coefficient (C_p) of main rotor (MR), tail rotor (TR), and total power coefficient with the advance ratio ($V/\Omega_0 R$) for a given blade loading ($Ct/\sigma=0.08$). The power consumed by the helicopter is initially large due to the high induced losses occurring at large induced rotor velocities near hover. This then alleviates as the advance ratio increases, since mean induced velocity decreases, up to a minimum. At this point, the power demand rises again due to the contribution of the parasitic drag at high flight velocities.

The power requirements estimated with HECTOR exhibit good correlation with the set of flight test data documented by Bousman *et al* [23]. The largest discrepancies are observed at high speed for both, main and tail rotor. This can be attributed to the uncertainty of the estimated fuselage aerodynamic maps used in HECTOR to calculate the parasitic drag, which is magnified with flight speed. This uncertainty can lead to a different flight trim state and thus to a different overall power at high-speed conditions. However, the maximum advance ratio simulated in the case studies is lower than 0.3 (66 m/s) and therefore these discrepancies have no effect on the overall mission results.

Engine performance simulation

A model of the General Electric T700-GE-700 engine which powers the UH-60A Black Hawk helicopter is developed in TURBOMATCH. This powerplant is a small turboshaft engine in the 1100-1350 kW class, equipped with a five-stage axial and a single-stage centrifugal compressor; a conventional annular combustion chamber; a two-stage axial gas generator turbine; and a two-stage uncooled power turbine [24,25]. A scheme of this engine is shown in Fig. 5.

The DP used to develop the engine model corresponds to the Maximum Continuous Power (MCP) rating at SL-ISA conditions (Table 2). The turbine cooling and engine bleeding mass flows are defined relative to the inlet mass flow rate, and the values are based on mass-flow functions specific of the T700-GE-700 engine employed by Ballin [24].

In order to ensure the engine model created is accurate enough to simulate the performance of the T700-GE-700 engine, steady-state performance maps collected in [24] were used for the model validation. These maps were created by a simulation software called GE status-81 developed by the engine manufacturer. This code is a comprehensive analysis-oriented model which is used for detailed representation of the engine thermodynamic cycle [24]. The maps considered herein provide the gas generator speed and shaft power as a function of the fuel flow at SL-ISA conditions (Fig. 6).

The agreement between the model and the software in terms of both gas generator speed and shaft power is good for the complete range of fuel flow rates provided by the manufacturer. This is especially critical for the analysis of helicopter performance, where high and low power conditions are expected at different phases of the mission. The results obtained from two previous simulations performed by Ballin [24] and Garavello *et al* [26] are also included in Fig. 6, and show similar trends to those obtained in this work.

Gaseous emissions prediction

In order to estimate the NO_x emissions produced during the helicopter operation, an engine combustor model was created in HEPHAESTUS after the T700-GE-700 combustion chamber architecture. The GE T700/CT7 engine family uses a straight-through annular combustion system of 12.5 cm in length with a machined ring film cooled construction and 12 low-pressure air blast fuel injectors [25]. The combustor geometry shown in Fig. 7 is implemented in the code through the definition of the volume and air mass flow distribution in four combustor regions: flame front (FF), primary zone (PZ), intermediate zone (IZ) and dilution zone (DZ).

The combustor dimensions implemented in the model were obtained from burner cross section plots provided by Monty *et al* [27], whilst the air flow distribution along the combustor is based on a combustor engine model proposed by Fakhre *et al* [28] for a General Electric T700 family engine.

The ability to predict the pollutant emissions of CO_2 and NO_x at different operating conditions must be verified in order to assess the adequacy of the emissions model. CO_2 production is coupled with fuel consumption through the combustion reaction stoichiometry. Since fuel consumption is well predicted by the model (Fig. 6), the CO_2 emissions will be properly predicted as well. However, NO_x production is affected by operating factors such as gas temperature and pressure, fuel type, equivalence ratio and residence time within the combustor [29]. Thus, the capability of the model to predict the NO_x formation has to be validated. To that end, the operating conditions of the experiments conducted by Cohen at the NASA Lewis Research Center for the General Electric T700/CT7 engine family combustor [25] were simulated in the HEPHAESTUS model. The experiments were performed for JP-4 and JP-5 fuels. The experimental results for the JP-5 are used for validation (Fig. 8) since this fuel has a hydrogen content similar to the Jet A fuel, which is the aviation working fuel in HEPHAESTUS.

The model is able to predict the trend of the NO_x emissions with variations in combustor inlet temperature (Fig. 8). Overall, a good agreement with the experimental results is observed and the NO_x production trend is accurately predicted by the simulation model. An error of 22% is observed at the lowest value of combustor inlet temperature (483 K), which corresponds to an engine power output of 35 kW. This relatively high discrepancy is not as relevant for the NO_x emissions prediction, since the helicopter powerplant rarely operates at such a low power setting. For the rest of points, the error in the NO_x prediction lies well below an acceptable 10%.

IMPACT OF OPERATIONAL CONDITIONS AND ENGINE DEGRADATION ON ROTORCRAFT PERFORMANCE CHARACTERISTICS

The effects of the environmental parameters considered in the present study i.e. ambient temperature and flight altitude, along with the compressor degradation on the rotorcraft-engine performance are presented in this section. The effect of helicopter All-Up Mass (AUM) in helicopter power demand is also included for the sake of completeness. In fact, the effect AUM has on helicopter power, affects indirectly the powerplant fuel consumption and the amount of NO_x emitted.

Firstly, the effect of flight altitude, ambient temperature and mass on the UH-60A Black Hawk power required is analyzed (Fig. 9). This change in power demand, motivated by the change in rotor thrust requirements, modifies the fuel consumption and NO_x emissions of the powerplant accordingly (Figs. 10 and 12). As a result of these fluctuations, the airspeed for maximum range and the airspeed for minimum NO_x formation vary as well (Figs. 11 and 13). The airspeed of minimum NO_x formation is defined in the context of the analysis as the air speed that minimizes the NO_x emitted at cruise per unit of distance travelled. The graphical derivation of these speeds at different ambient temperatures, flight altitudes and helicopter AUMs is shown in Figs. 11 and 13, and their values listed in Table 3.

The aspect of the power curves shown in Fig. 9 corresponds to the classic 'bucket-shape' curve characteristic of the rotorcraft power (main rotor power plus tail rotor contribution). At low speeds, the power demand is driven by the induced term, whilst at high speeds the parasitic drag of the fuselage is the dominant component [1]. Induced power decreases with air density, whilst the parasitic term increases. However, the parasitic power, which is a result of the fuselage drag, is mainly dependent on the helicopter airspeed, and the effect of density is not as relevant as it is for the induced power. Therefore, the fluctuations in air density caused by changes in ambient temperature and flight altitude will mainly affect the induced component of the helicopter power.

Air density reduces as temperature or flight altitude increases, and vice versa. Thus, at lower airspeeds the lower density results in a higher power because of the increment in induced power, whilst at higher airspeeds the power required is reduced due to the reduction in parasitic drag (Fig. 9.a).

An increase in flight altitude has a similar effect on the helicopter power requirement: this parameter increases at low speeds with altitude, and reduces at higher speeds (Fig. 9.b). In this case, it must be noted that the fluctuation in air density is higher with altitude than with ambient temperature, which translates in a greater

change in induced power and thus, a higher power variation at lower speeds. An additional increase in power demand is observed at a certain airspeed band (10-30 m/s) for a flight altitude of 4500 m (Fig. 9.b). This phenomenon is due to the impingement of the rotor wake on the horizontal stabilizer, causing the fuselage nose to pitch-up, and requiring a subsequent trim correction from the pilot.

Regarding the effect of helicopter mass, an increase in AUM translates in a rise in helicopter induced power. Therefore, the effect of AUM is most pronounced at the low speed range, where the induced power term constitutes a greater fraction of the total rotorcraft power requirement (Fig. 9.c).

The powerplant fuel flow is proportional to the rotorcraft power (Fig. 10). This is clearly shown in Fig. 10.c where the effect of helicopter AUM is considered. Regarding ambient temperature and flight altitude, they not only affect the main rotor power required for a given thrust, but also the thermal efficiency of the powerplant (Figs. 14.a and 14.b). Thus, the analysis of the impact of the environmental conditions on rotorcraft performance constitutes a multi-disciplinary problem which involves the effect on rotorcraft aerodynamic performance on one hand, and the effect on engine aero-thermal performance in the other hand. The fuel flow trends observed in Figs. 10.a and 10.b are driven by the two mentioned effects.

The slightly positive effect the drop in ambient temperature has on engine fuel consumption (Fig. 14.a) together with the lower power requirement makes the fuel flow to reduce at low airspeeds. At higher speeds, the increase in engine thermal efficiency with lower ambient temperature is offset by the increase in helicopter power requirement, and thus the global effect of ambient temperature in fuel consumption is reduced at high helicopter airspeeds.

About flight altitude, this parameter has a more significant effect on engine efficiency (Fig. 14.b), and so its influence on the fuel flow rate in forward flight is more evident (Fig. 10.b). Since engine fuel flow is reduced with altitude, the power increase at low air speed is moderately balanced out, whilst the reduction in power at high speeds leads to an even greater reduction in fuel consumption.

The variations in engine fuel flow caused by temperature, altitude and helicopter AUM inevitably affect the value of the air speed for maximum range. This variation is graphically shown in Fig. 11, and the speed values at different conditions listed in Table 3. Figure 11 shows the powerplant fuel flow divided by the helicopter airspeed, w_f/V, versus airspeed at different ambient temperatures, flight altitudes and helicopter AUMs. This parameter offers a measure of the fuel consumed by the helicopter per unit of distance flown. This way, the airspeed of maximum range is easily identified in the graph as the airspeed that minimizes the ratio

w_f/V (black dot). Figure 11 indicates that the higher the ambient temperature, flight altitude and helicopter AUM, the higher the airspeed for maximum range. It is emphasized that for the range of conditions simulated, flight altitude and helicopter mass have a greater impact on airspeed for maximum range than ambient temperature.

The effect of ambient temperature, flight altitude and helicopter AUM on NO_x emissions rate in forward flight is shown in Fig. 12. Similarly to engine fuel flow, NO_x production is also proportional to engine shaft power as it is observed in Fig. 12.c where the effect of helicopter AUM is displayed. Concerning the effect of ambient temperature and flight altitude, it represents a multi-disciplinary problem as well, since not only the aerodynamic performance of the rotorcraft is affected, but also the operating conditions at the powerplant combustors.

The rise in ambient temperature amplifies the NO_x formation at high power settings (Fig. 15.a). This effect causes that, despite of the power reduction observed at high air speeds with the rise in ambient temperature (Fig. 9.a), the final NO_x production rate is above the standard ISA case. As a result of this behavior, the NO_x rate at any flight speed increases with a rise in ambient temperature, and vice versa.

Considering the effect of flight altitude in the NO_x emissions rate (Fig. 12.b), it is observed that an increase in the altitude level comes with a reduction in the formation of NO_x, all along the helicopter air speed range. Regardless of the increased helicopter power at low air speed due to the rise in altitude (Fig. 9.b), the descent in NO_x production with altitude (Fig. 15.b) dominates and so, the NO_x rate reduces. At high flight speeds, the drop in power requirement enhances the reduction in NO_x emissions which leads to a decrement around 50% for a flight speed of 60 m/s at a flight altitude of 4500 m. The previous statement is generally true except in the speed band where the abnormal increase in rotor power was observed at 4500 m altitude (Fig. 9.b). Over this speed range, the additional increase in helicopter power requirement triggers the formation of NO_x slightly above the level expected at those conditions.

The variations of the airspeed for minimum NO_x formation with ambient temperature, flight altitude and helicopter AUM are graphically presented in Fig. 13 and summarized in Table 3. Figure 13 displays the powerplant NO_x production rate divided by the helicopter air speed, w_{NOx}/V, versus airspeed at different ambient temperatures, flight altitudes and helicopter AUMs. Similar to the analysis of the airspeed for maximum range, this magnitude offers a measure of the NO_x emitted by the helicopter powerplant per unit of distance flown.

Thus, the airspeed for minimum NO_x can be pinpointed as the airspeed that minimizes the ratio w_{NOx}/V (black dot).

The higher the flight altitude and helicopter AUM, the higher the airspeeds for minimum NO_x formation. However, it has been observed that when the ambient temperature deviates from the standard ISA value, the speed for minimum NO_x formation increases, regardless the direction (positive or negative) of the ambient temperature variation. In common with the airspeed for maximum range, flight altitude and helicopter AUM have a greater impact on the airspeed for minimum NO_x formation than ambient temperature.

Results in Table 3 show that the airspeed for maximum range is generally higher than the airspeed for minimum NO_x formation. This result implies that is not possible for the helicopter to fly at a cruise speed that at the same time minimizes engine fuel burn and NO_x emissions, and so, a trade-off between these two parameters and final mission time must be always assumed. Assuming a mission length of 100 km and a flight speed of 50 m/s, a difference in 5 m/s (order of magnitude of the discrepancies observed in Table 3) will cause a difference of about 3.5 minutes in the total mission time.

The effect of altitude, temperature and compressors degradation on the GE T700-GE-700 engine performance is shown in Figs. 14 and 15. The compressor deterioration was simulated with an isentropic efficiency (η) and flow capacity (Γ) degradation of 2.5% and 5%, respectively. These values are similar to those used in the case study shown in the next section and are based on typical values detected in real engines [30] . It was assumed that both axial and radial compressors were equally degraded.

Engine fuel flow is slightly affected by the ambient temperature due to the changes in the work required by the compressor with inlet air temperature. The fuel flow in hot environmental conditions is larger than the fuel flow at colder conditions since the compression work is higher and vice versa (Fig. 14.a). However, the effect of altitude on fuel flow is more relevant (Fig. 14.b). As a result of the pressure drop at the engine inlet with altitude, the engine works with an increased pressure ratio which translates in a gain in cycle efficiency and so, a reduction of the fuel consumption. Compressor degradation, as expected, has a negative effect on the engine efficiency. The reduction in flow capacity of the degraded component requires an increase in specific power in order to deliver the same shaft power. This increase in specific power is achieved by burning extra fuel in order to rise the TET. Together with this effect, the reduction of the compressor efficiency impairs the cycle efficiency, which further contributes to the total fuel flow increase.

NO_x emissions, as they are computed in the present analysis, depend on the air conditions at the inlet of the combustor, the airflow supply going into the burner and the amount of fuel employed in the combustion. Therefore, to explain the behavior of NO_x with ambient temperature, the combustor inlet temperature trend is plotted (Fig.16). The increase in this parameter with the ambient temperature, together with the slightly increase in fuel flow (Fig. 14.a) explains the trend observed in (Fig. 15.a). The influence of altitude in the NO_x emissions is shown in Fig. 15.b. The combined effect of pressure and air flow drop at the inlet of the combustor (Fig. 17) added to the effect of fuel reduction with flight altitude (Fig. 14.b) explains the reduction of NO_x production with flight altitude. It is emphasized that the effect of altitude on the NO_x rate is more sizeable than the effect of ambient temperature.

The effect of compressor degradation on NO_x emissions (Fig. 15.c) is small compared with flight altitude or ambient temperature. The change in combustor inlet conditions i.e. air pressure and temperature, are almost negligible and only fuel flow (Fig. 14.c) and airflow are slightly affected.

For the degraded engine it is observed that NO_x emissions are slightly lower at low power settings and become higher towards the end of the power curve. This behavior can be explained by the distribution of flame temperature and equivalent ratio of the combustor Flame Front and Primary Zone (Fig. 18). These are the two parts of the combustor responsible for the NO_x production since the flame temperatures observed in these regions are high enough to trigger the NO_x formation mechanisms. It is observed that the equivalent ratio in the FF region is above the stoichiometric value, and so, the increase in fuel flow of the degraded engine contributes to slightly lower the flame temperature.

On the other hand, the equivalent ratio on the PZ is below the stoichiometric value, which implies, that the increase in fuel contributes to rise the flame temperature in this region. The flame temperature of the PZ is much lower at low power settings than the temperature at the FF, and so is its contribution to the NO_x formation. That explains that the trend in Fig. 15.c. at low shaft power is dominated by the slight reduction in flame temperature at the FF.

However, the temperature at the PZ rises continuously (Fig. 18), which causes a change in trend in the NO_x rate at a shaft power around 700 kW. At this point, the production of this pollutant in the PZ becomes significant and its relevance in the total NO_x account increases. As the flame temperature in the PZ in the degraded engine is higher (Fig. 18), the NO_x production rate is also higher, and as a result, at the end of the power spectrum an increase of NO_x formation is observed for the degraded engine.

MISSION LEVEL CASE STUDY DEFINITION

The helicopter model described in previous sections is used to assess the overall impact of the environmental conditions on helicopter performance at mission level. Particularly, the effects of high temperature, dust ingestion, and high altitude on fuel consumption and NO_x production are evaluated. Two missions are envisioned for this purpose. Firstly, a theoretical EMS mission over a hot desert area is designed to assess the effect of high temperature and compressor degradation. Secondly, a SAR mission over an elevated cold area ('High & Cold' scenario) is considered so as to evaluate the effect of low temperature and low air density on helicopter operation.

Emergency Medical Service (EMS) mission

The scenario chosen for the hypothetical EMS mission is situated in the Mojave Desert area. In particular, the helicopter is considered to take-off from the Palm Springs International Airport, California, to pick-up several civilians in distress from an accident location in the Joshua Tree National Park, and transport them to the Robert E. Bush Naval Hospital in Twentynine Palms, California. The geographical trajectory of the mission in global coordinates is reproduced in Fig. 19.a. The mission altitude and airspeed profiles are shown in Fig. 19.b. It is observed that the mission comprises three legs. The flight altitude of each corresponds to an AGL average altitude of 450 m, bearing in mind the ground altitude fluctuations along the flight path. The cruise speed for the three legs is 60 m/s. Climb and descent rates are held fixed at 5m/s, and the idle segments are assumed to be operated at 20% of DP (Maximum Continuous Power) engine shaft power. A hover segment of 60 seconds duration is completed before any climb maneuver and at the end of the mission. The mission payload breakdown is detailed in Table 4.

The arid nature of the Joshua Tree National Park and its surroundings together with the high temperatures justify the selection of this location to simulate the hot sandy desert conditions. Particularly, the temperature and engine degradation conditions summarized in Table 5 are simulated. The mission was first simulated at ISA and clean engine conditions. Then, the temperature was modified to assess the effect of hot temperature on helicopter performance. The value of ISA +24 is based on the average high temperature in July (most torrid month) measured in Twentynine Palms according to US Climate Data (39°C, 103°F) [31]. Finally, the sand and dust ingestion effects are added as engine compressors performance deterioration. A certain amount of these particles manages to get through the filtration system and deposits on compressor blades reducing efficiency, η, and mass flow capacity, Γ. This deterioration cause is known as fouling and is more commonly observed in compressor rather than turbine components. Therefore, two different pair of compressor degradation levels were

considered in the analysis based on engineering judgment and typical values detected in real engines [30]. It was assumed that both axial and radial compressors were equally degraded.

Search and Rescue (SAR) mission

For the SAR mission the helicopter was considered to complete a research pattern in the Rocky Mountains region. To that end, the helicopter takes-off from the Rose Medical Center Heliport in Denver, Colorado. From this location the helicopter transits to the Mt. Evans where it performs a circular search pattern of 5 km radius. After this first loop the helicopter moves towards a mountain resort nearby where it repeats the same searching maneuver until the civilians in distress are found and collected. The helicopter transits then back to the hospital of origin where the rescued civilians receive medical attention (Figs. 20.a and 20.b). In this case, the mission includes three cruise legs and two loiter segments. As in the EMS mission, the cruise segments are operated at around 450 m AGL and 60 m/s, and same assumptions were kept for the climb, descent and idle segments. The loiter leg is flown at a reduced altitude of 60 m and at 30 m/s, and the helicopter hovers for 10 minutes during the rescue operation. The mission payload breakdown is detailed in Table 6.

The elevation of the region and its climate are ideal to analyze the effect of high altitude and low temperature conditions on helicopter performance. The average elevation of the area covered by the helicopter trajectory is around 2800 m (9185ft) whilst the temperature considered is ISA -23 (18°F). This value of temperature is based on the average low temperature in January (coolest month) registered in Denver by US Climate Data (-8°C , 18°F) [32]. To quantify the effects of the environmental conditions on helicopter fuel consumption and emissions, the results obtained under these particular conditions of altitude and temperature are benchmarked against the results produced by the simulation of the same helicopter trajectory at standard temperature and SL conditions. The mission altitude and airspeed profiles are reproduced in Fig. 20.c. Same operational procedures were applied for the benchmark mission. As a consequence of the increased flight altitude, the helicopter spends more time in climb and descent under the 'High & Cold' scenario. Therefore the mission times are slightly different for each scenario, namely, 5220 seconds (87 min) for the SL scenario and 5490 seconds (91.5 min) for the 'High & Cold' scenario.

MISSION LEVEL ANALYSIS: ASSESSMENT OF OPERATIONAL PERFORMANCE AND ENVIRONMENTAL IMPACT

The results obtained for the EMS missions are first presented in Table 7 and Figs. 21 and 22. Note that the results of shaft power, fuel flow and NO_x emissions in Figs. 21 and 22 are values per engine. As a consequence

of the high temperature (Case 2), the mission fuel and NO_x emissions increase compared with the reference mission (case 1). The addition of compressor degradation (Cases 3 and 4) further increases the mission fuel, whilst it slightly reduces overall NO_x emissions in comparison with Case 2.

In agreement with the trend observed in Fig. 9.a, the rise in ambient temperature reduces the power required by the main rotor at cruise (V=60 m/s), whilst the power demand at hover is increased (Fig. 21.a). In the descent and climb segments, where the effect of the thinner atmosphere prevails over the reduction in airframe drag, the rise in ambient temperature also translates in a slightly higher power demand. This fluctuation in the main rotor power directly affects the fuel consumption as engine fuel flow is proportional to the shaft power (Fig. 14). Apart from the effect on main rotor performance, the higher ambient temperature also impairs the engine efficiency (Fig. 14.a), which shifts the fuel flow trend up (Fig. 21.b) and balances out the effect of reduced main rotor power at cruise conditions. Therefore, the overall effect of the ambient temperature rise is an increase in the mission block fuel as seen in Table 7. However, the magnitude of this effect is mission dependent, as missions with longer cruise segments will be less penalized in fuel consumption than those with a high number of climb & descent cycles.

NO_x emissions, like fuel flow, are proportional to shaft power (Fig. 15), and so a similar trend is observed for the NO_x production over the mission (Fig. 21.c). Equally to the fuel flow distribution, the rise in ambient temperature has also a negative effect on the NO_x production rate (Fig. 15.a), and so, the overall emissions are penalized as shown in Table 7.

When compressor degradation is considered, the fuel flow at each flight segment increases (Fig. 22.a). This result is directly linked with the fuel flow distribution observed in Fig. 14.c and explains the increase in mission fuel for Cases 3 and 4 observed in Table 7. Regarding the NO_x production over the mission (Fig. 22.b), it is observed that compressor degradation only increases the emissions with respect to the clean configuration in those segments with a high power demand, i.e. the four hover segments and the second climb segment (after collection of the civilians in distress). On the other hand, in those segments with a low power consumption, such as descent and idle, the NO_x production rate of the degraded configuration is lower. This distribution of the NO_x emissions over the mission is in agreement with the trend previously obtained for the effect of compressor degradation on NO_x formation (Fig. 15.c). For the particular mission simulated, the helicopter spends more time in descent and idle conditions than at hover; therefore the NO_x production is reduced compared with the clean engine configuration. However, this cannot be generalized, since the same flight path operated with an increased

payload or an alternative flight path with a different proportion of hover segments and idle/descent segments may generate a different NO_x emissions response.

The results obtained for the SAR mission at the two different scenarios simulated are presented in Table 8 and Fig. 23. As before, the results in Fig. 23 refer to values per engine.

In the 'High & Cold' scenario simulated, the high altitude and low temperature have opposed effects on the helicopter power. In fact, lower temperatures imply a denser atmosphere, whilst the opposite is achieved with the increase in flight altitude. From the two effects, the contribution of flight altitude to helicopter power demand is dominant (Fig. 9). Therefore, for the 'High & Cold' mission the helicopter power in those segments driven by the induced power (hover, climb and descent) is higher, whilst at cruise, where the parasitic drag is the dominant effect, the power demanded by the helicopter is lower (Fig. 23.a). In contrast to the operation at cruise, the power required to fly the loiter segments is higher for the 'High & Cold' scenario, due to the reduced loiter airspeed (Figs. 20.b and 20.c). In fact, at the loiter speed (V=30m/s), the power consumed by the main rotor is still governed by the induced term (Fig. 9). Note that a non-dimensional time has been used to plot Fig. 23 since the two scenarios have a slightly different mission duration.

Regarding the operation of the engine, the high altitude and low temperature of the 'High & Cold' scenario have a positive effect on the engine fuel consumption (Figs. 14.a and 14.b). This increase in engine efficiency translates in a fuel flow reduction in all the mission segments. For the particular combination of temperature and altitude of the mission simulated, it is observed that the engine efficiency offsets the power increase in those aforementioned segments, whilst the combined effect of reduced main rotor power and improved engine efficiency translates in a sizeable 20% fuel reduction on the cruise segment (Fig. 23.b). This fuel consumption distribution over the mission explains the results shown in Table 8. Similar comments apply for the NO_x production along the mission (Fig. 23.c). The low temperature and high altitude combination impairs the formation of NO_x in the combustor (Fig. 15.a and 15.b), resulting in the overall emission reduction observed in Table 8.

CONCLUSIONS

This paper described the effects of environmental conditions on the performance of a TEM helicopter at rotorcraft and mission level. A multidisciplinary helicopter flight performance simulation framework developed and validated at Cranfield University has been utilized to simulate the different aspects of the helicopter operation. The reference helicopter implemented in the code has been modeled after the Sikorsky UH-60A

Black Hawk. The different components of the helicopter model have been described and validated against experimental and manufacturer data.

Firstly, the response to changes in ambient parameters on helicopter performance in forward flight was analyzed. Helicopter AUM was also considered here for completeness. The impact on aircraft-engine performance characteristics and gaseous emissions were extensively evaluated at aircraft level. For the range of conditions considered in the study, flight altitude and helicopter mass showed to be the dominant parameters in terms of their effect on rotorcraft performance. Variations of the airspeed for maximum range of 11% and 17%, and 7.5% and 7% for minimum NO_x formation were attained with changes in flight altitude and AUM, respectively. The results showed the necessity to assume a trade-off between fuel and NO_x minimization, since the optimum speed for fuel is generally higher than the optimum speed for NO_x (difference not higher than 5m/s).

The mission level analysis was conducted over two case studies: an EMS and a SAR mission, where the effects of ambient temperature, flight altitude and compressors degradation were assessed.

For the EMS mission, the negative effect of high temperature in fuel consumption and NO_x emissions was highlighted, despite of the reduction in helicopter power observed at cruise conditions. As a result, an increase in mission fuel of 2% was obtained for the hotter scenario. Compressor degradation further increases the mission fuel by an additional 3% (for the most severe degradation case), although its effect on NO_x formation may be regarded as negligible. At the particular conditions simulated herein, a slightly reduction in mission NO_x was obtained, but the positive or negative contribution of compressor degradation to the NO_x account was shown to be dependent on the level of shaft power required by the main rotor.

Regarding the SAR mission, it has been highlighted that the effect of altitude on the helicopter power is dominant over the effect of temperature. Therefore, under realistic ambient temperature fluctuations, the power consumed by the helicopter will be driven by flight altitude (ambient pressure), in such a way that the power consumed in segments driven by the parasitic drag will drop with altitude, and the opposite will occur for segments driven by the induced term. It has been also shown that the high altitude and low temperature combination has positive effects on fuel consumption and NO_x production offsetting the increased power in hover, climb, descent and loiter in the particular mission, and leading to a reduction of 12% and 40% in mission fuel and NO_x, respectively.

The present work provides insight of the extent the design performance of a given helicopter is affected by the environmental conditions of the operational scenario. This constitutes a multi-disciplinary problem which involves the impact on rotorcraft aerodynamics and the effect on the powerplant performance. The results obtained throughout the analysis presented herein suggest that the operational conditions surrounding the helicopter cannot be neglected if the environmental sustainability of the helicopter is to be thoroughly assessed. The effect of the operating conditions on the airspeed for maximum range and the airspeed for minimum NO_x formation also highlights the need for adapting the helicopter operation to the mission scenario conditions and the payload requirements in order to minimize its environmental impact. The findings presented complement the research already developed on rotorcraft performance assessment and optimization.

REFERENCES

[1] Gordon Leishman, J., 2006, *Principles of Helicopter Aerodynamics*, 2nd Edition, Cambridge University Press.

[2] Rindlisbacher, T., 2009, "Guidance on the Determination of Helicopter Emissions," Federal Office of Civil Aviation (FOCA), Division Aviation Policy and Strategy, Bern (Switzerland), Reference No. 0/3/33/33-05-20.

[3] MacMillan, W. L., 1974, "Development of a Modular Type Computer Program for the Calculation of Gas Turbine Off Design Performance," Ph.D. thesis, Department of Power and Propulsion, Cranfield University.

[4] Celis, C., 2010, "Evaluation and Optimisation of Environmentally Friendly Aircraft Propulsion Systems," Ph.D. thesis, School of Engineering, Cranfield University.

[5] Goulos, I., 2012, "Simulation Framework Development for the Multidisciplinary Optimisation of Rotorcraft," Ph.D. thesis, School of Engineering, Cranfield University.

[6] "Sikorsky BLACK HAWK Helicopter," 2016. Available: http://www.lockheedmartin.com/us/products/h-60-black-hawk-helicopter.html. [Accessed: 19-Nov-2016].

[7] Goulos, I., Fakhre, A., Tzanidakis, K., Pachidis, V., and D'Ippolito, R., 2015, "A Multidisciplinary Approach for the Comprehensive Assessment of Integrated Rotorcraft–Powerplant Systems at Mission Level," *J Eng Gas Turb Power*, vol. 137, no. 1, pp. 12603.

[8] Goulos, I., Hempert, F., Sethi, V., Pachidis, V., D'Ippolito, R., and D'Auria, M., 2013, "Rotorcraft Engine Cycle Optimization at Mission Level," *J Eng Gas Turb Power*, vol. 135, no. 9, p. 091202.

[9] Fakhre, A., Tzanidakis, K., Goulos, I., Pachidis, V., and D'Ippolito, R., 2015, "Multi-Objective Optimization of Conceptual Rotorcraft Powerplants: Trade-off Between Rotorcraft Fuel Efficiency and Environmental Impact," *J Eng Gas Turb Power*, vol. 137, no. 7, p. 071201.

[10] Goulos, I., Pachidis, V., D'Ippolito, R., Stevens, J., and Smith, C., 2012 "An Integrated Approach for the Multidisciplinary Design of Optimum Rotorcraft Operations," *J Eng Gas Turb Power*, vol. 134, no. 9, pp. 349–361.

[11] Linares, C., Lawson, C. P., and Smith, H., 2013, "Multidisciplinary Optimisation Framework For Minimum Rotorcraft Fuel and Air Pollutants at Mission Level," *Aeronautical Journal*, vol. 117, no.

1193, pp. 749–767.

[12] Goulos, I., Pachidis, V., and Pilidis, P., 2014, "Lagrangian Formulation for the Rapid Estimation of Helicopter Rotor Blade Vibration Characteristics," *Aeronautical Journal*, vol. 118, no. 1206, pp. 861–901.

[13] Peters, D. A., Boyd, D. D., and He, C. J., 1989, "Finite-State Induced-Flow Model for Rotors in Hover and Forward Flight," *Journal of American Helicopter Society*, vol. 34, no. 4, pp. 5–17.

[14] Leishman, J. G. and Beddoes, T. S., 1989, "A Semi-Empirical Model for Dynamic Stall," *Journal of American Helicopter Society*, vol. 34, no. 3, pp. 3–17.

[15] Cheeseman, I. C. and Bennett, W. E., 1957, "The Effect of the Ground on a Helicopter Rotor in Forward Flight,", no. 3021, Aeronautical Research Council.

[16] Padfield, G. D., 2007, *Helicopter Flight Dynamics*, 2nd edition. London: Blackwell Science.

[17] Pitt D. M. and Peters, D. A., 1980, "Theoretical Prediction of Dynamic-Inflow Derivatives," *Sixth European Rotorcraft and Powered Lift Aircraft Forum*, no. 47.

[18] European Organization for the Safety of Air Navigation (Eurocontrol) and Institute of Geodesy and Navigation (IfEN), 1998, "WGS 84 Implementation Manual," Brussels (Belgium).

[19] Li, Y., Marinai, L., Pachidis, V., Lo Gatto, E., and Philidis, P., 2009, "Multiple-Point Adaptive Performance Simulation Tuned to Aeroengine Test-Bed Data," *Journal of Propulsion and Power*, vol. 25, no. 3, pp. 635–641.

[20] Pachidis, V., Pilidis, P., Marinai, L., and Templalexis, I., 2007, "Towards a full two dimensional gas turbine performance simulator," *Aeronautical Journal*, vol. 111, no. 1121, pp. 433–442.

[21] Johnson, W., 2010, "NDARC - NASA Design and Analysis of RotorCraft Validation and Demonstration," AHS Aeromechanics Specialists Conference 2010, no. February, pp. 804–837.

[22] Hamade, K. S. and Kufeld, R. M., 1990, "Modal Analysis of UH-60A Instrumented Rotor Blades," NASA-TM 4239, NASA Ames Research Center.

[23] Bousman, W. G. and Kufeld, R. M., 2005, "UH-60A Airloads Catalog," NASA-TM 2005-212827, NASA Ames Research Center.

[24] Ballin, M. G., 1988, "A High Fidelity Real-Time Simulation of a Small Turboshaft Engine," NASA-TM 100991, NASA Ames Research Center.

[25] Cohen, J. D., 1983, "Analytical Fuel Property Effects - Small Combustors Phase I," NASA-CR 168138, NASA Lewis Research Center.

[26] Garavello, A. and Benini, E., 2012, "Preliminary Study on a Wide-Speed-Range Helicopter Rotor/Turboshaft System," *Journal of Aircraft*, vol. 49, no. 4, pp. 1032–1038.

[27] Monty, J. and Scott, T., 1985, "Analytical Fuel Property Effects - Small Combustors Phase II," NASA-CR 174848, NASA Lewis Research Center.

[28] Fakhre, A., Pachidis, V., and Pervier, H., "NOx Emissions Prediction for GE T700-T6A Type Combustor Using a Physics-Based Multi-Reactor Model," Department of Power and Propulsion, Cranfield University.

[29] Lefebvre, A. H. and Ballal, D. R., 2010, *Gas Turbine Combustion: Alternative Fuels and Emissions*, 3rd Edition, CRC Press.

[30] Litt, J., Parker, K., and Chatterjee, S., 2003, "Adaptive Gas Turbine Engine Control for Deterioration Compensation Due to Aging," TM-2003-212607, NASA Glenn Research Center.

[31] "U.S. climate data," 2016. Available: http://www.usclimatedata.com/climate/twentynine-palms/california/united-states/usca1173. [Accessed: 11-Nov-2016].

[32] "U.S. climate data," 2016. Available: http://www.usclimatedata.com/climate/denver/colorado/united-states/usco0501. [Accessed: 11-Nov-2016].

Table 1 Rotorcraft model design parameters [21]

Empty weight [kg]	5082
Solidity, σ [-]	0.089
Number of blades [-]	4
Blade radius, R [m]	8.178
Blade chord [m]	0.527
Blade airfoils	SC1095 & SC1094 R8
Equivalent blade twist [deg]	18
Nominal rotor speed, Ω_0 [rad/s]	27.01

Table 2 Engine model design point at MCP SL-ISA conditions

Inlet pressure recovery [-]	0.986
Design mass flow [kg/s]	4.170
Compressor section	
Axial compressor PR [-]	5.3
Centrifugal compressor PR [-]	2.8
Axial compressor η [-]	0.821
Centrifugal compressor η [-]	0.821
Cooling flow bleed percentage [%]	8.46
Engine bleed percentage [%]	1.06
Combustion section	
Combustion efficiency [-]	0.984
Combustor pressure drop [%]	4.0
TET [K]	1440
Fuel flow [kg/s]	0.0807
Turbine section	
Gas generator turbine η [-]	0.852
Free power turbine η [-]	0.845
Shaft power [kW]	987.0

Table 3 Variation of optimum air speeds for fuel and NO_x

	Fuel flow rate		NO_x rate	
	V_{rg} [m/s]	$\Delta\%$ V_{rg}	V_{NOx} [m/s]	$\Delta\%$ V_{NOx}
Ambient temperature				
ISA	51.8	-	47.9	-
ISA +20	53.4	3.09	48.9	2.09
ISA -20	50.4	-2.70	50.0	4.38
Flight altitude				
SL	51.8	-	47.9	-
1500 m	52.9	2.12	51.7	7.93
4500 m	57.5	11.00	56.1	17.12
Helicopter AUM				
7000 kg	52.1	-	50.7	-
8000 kg	53.9	3.45	52.6	3.75
9000 kg	56.0	7.49	54.3	7.10

Table 4 EMS mission payload breakdown

Payload type	Quantity	Weight [kg]
Stretcher	6	300
Medical attendant	1	90
Medical assistant	1	90
Patient	3	270
Medical equipment	-	300
Total weight		1050

Table 5 EMS mission simulation cases

Case	ISA deviation	Compressor degradation	
		$\Delta\eta$ (%)	$\Delta\Gamma$ (%)
1	0	0	0
2	+24	0	0
3	+24	-1.25	-2.5
4	+24	-2.5	-5

Table 6 SAR mission payload breakdown

Payload type	**Quantity**	**Weight [kg]**
Medical attendant	1	90
Medical assistant	1	90
Civilians	8	720
Rescue equipment	-	50
Total weight		950

Table 7 EMS mission total fuel burn and NO_x emissions results

Case	Fuel [kg]	NO_x [kg]	%Δ Fuel	%Δ NO_x
1	269.3	1.210	-	-
2	274.7	1.298	2.02	7.32
3	279.2	1.291	3.68	6.73
4	283.7	1.290	5.37	6.63

Table 8 SAR mission total fuel burn and NO_x emissions results

Case	Fuel [kg]	NO_x [kg]	%Δ Fuel	%Δ NO_x
ISA/SL	443.9	2.249	-	-
High & Cold	391.1	1.358	-11.89	-39.60

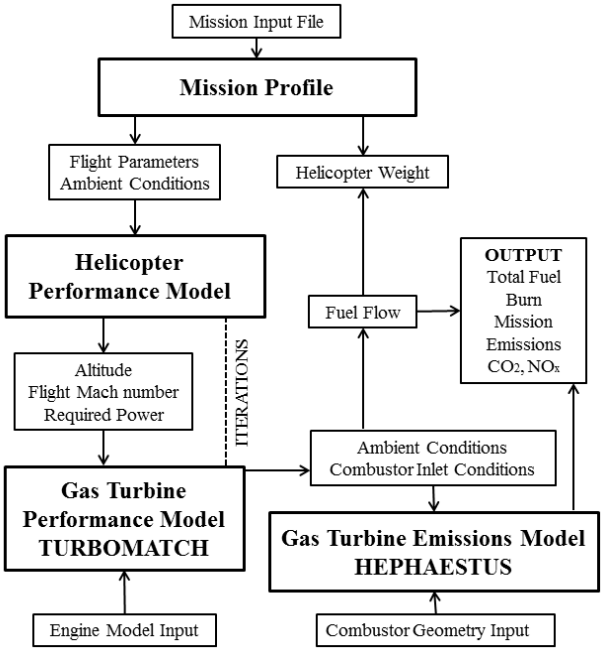

Figure 1 HECTOR architecture scheme [9]

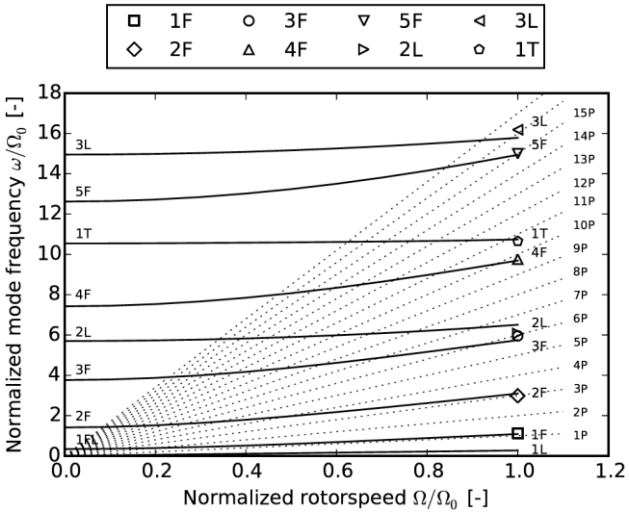

Figure 2 Resonance chart of the Sikorsky UH-60A main rotor

a)

b)

c)

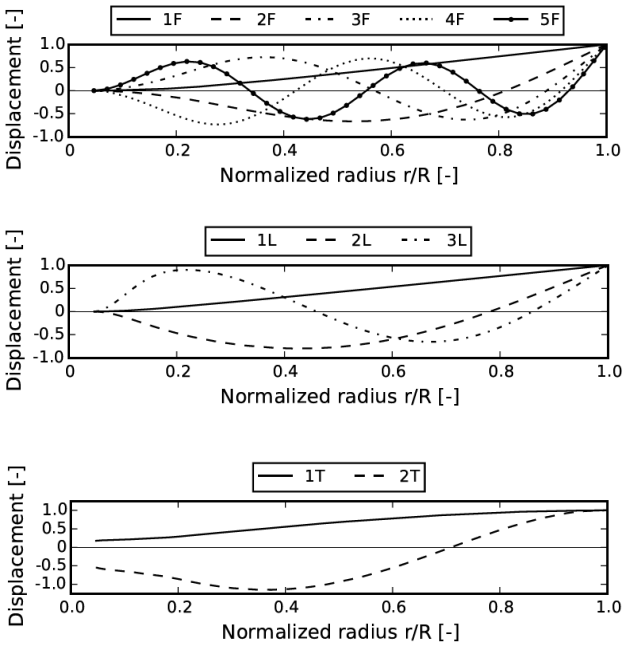

Figure 3 Shape of the main rotor vibration modes, Ω_0=27.01 rad/s: (a) Flap mode, (b) Lag mode, (c) Torsion mode

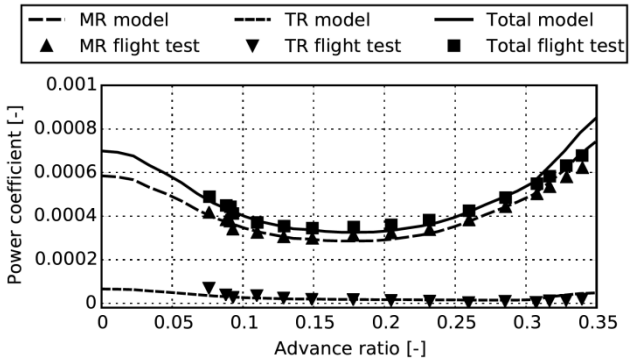

Figure 4 Rotorcraft model flight dynamics trim results

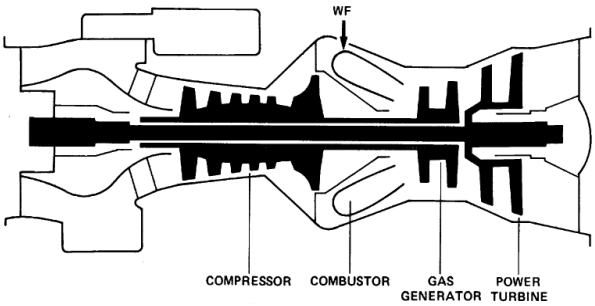

Figure 5 GE T700-GE-700 turboshaft engine layout [24]

a)

b)

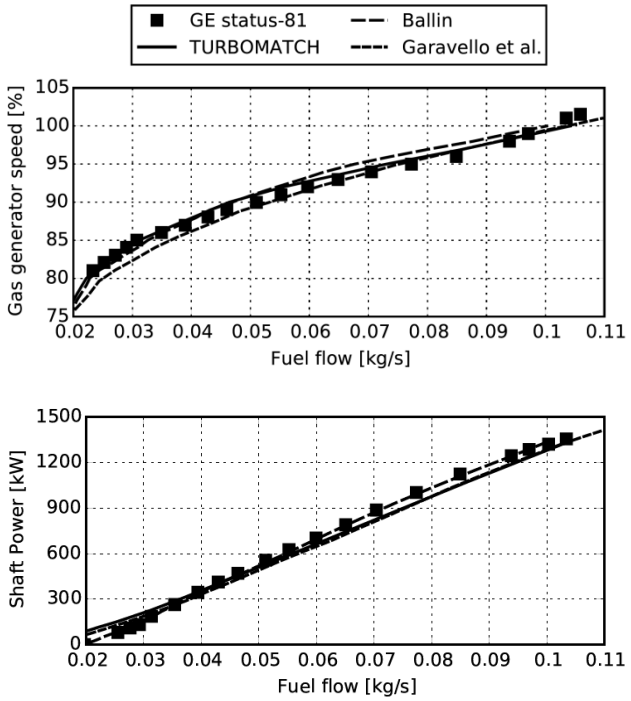

Figure 6 TURBOMATCH engine model validation: (a) gas generator speed vs. fuel flow, (b) shaft power vs. fuel flow

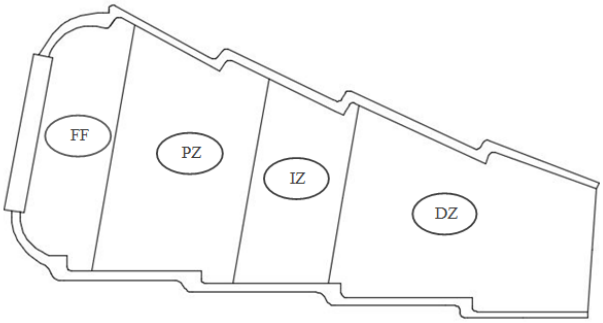

Figure 7 GE T700-GE-700 engine combustor layout

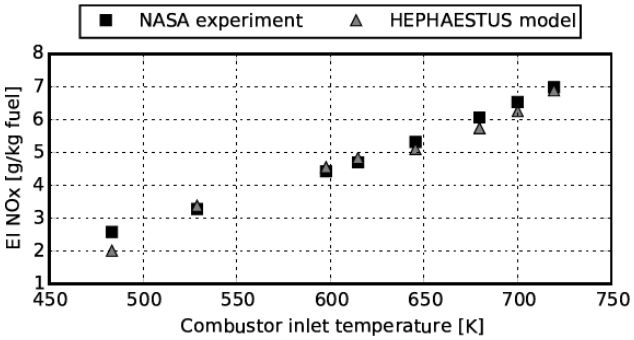

Figure 8 HEPHAESTUS emission model results comparison: EI NO_x vs. combustor inlet temperature

a)

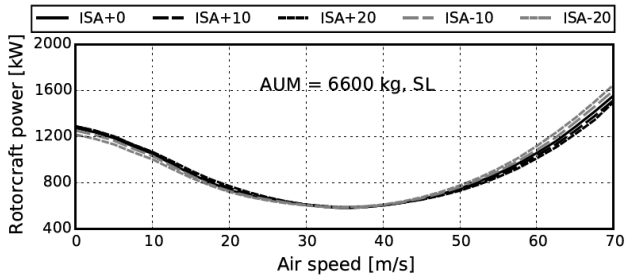

b)

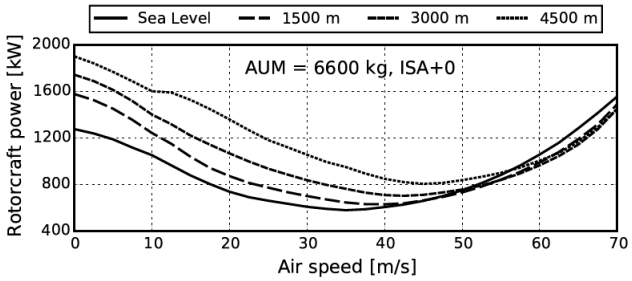

c)

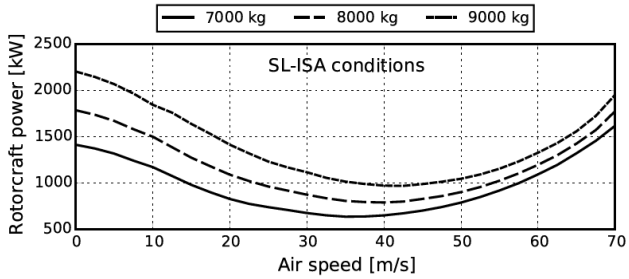

Figure 9 Helicopter power demand in forward flight at different: (a) ambient temperature, (b) flight altitude, (c) helicopter AUM

a)

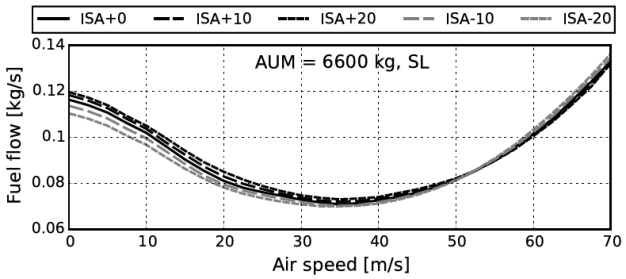

b)

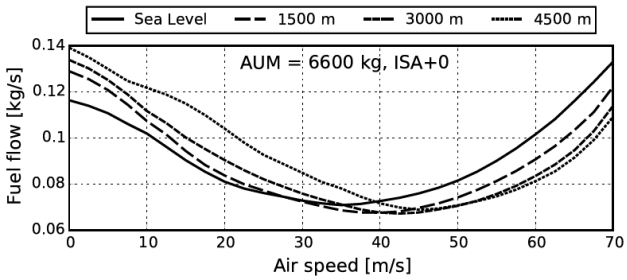

c)

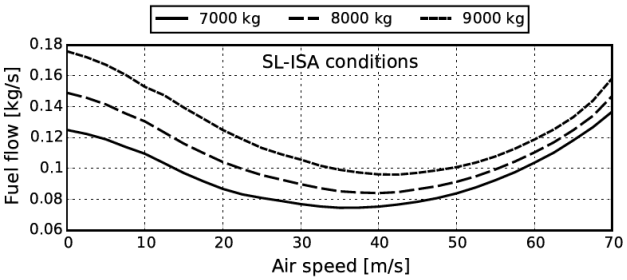

Figure 10 Powerplant fuel flow rate in forward flight at different: (a) ambient temperature, (b) flight altitude, (c) helicopter AUM

a)

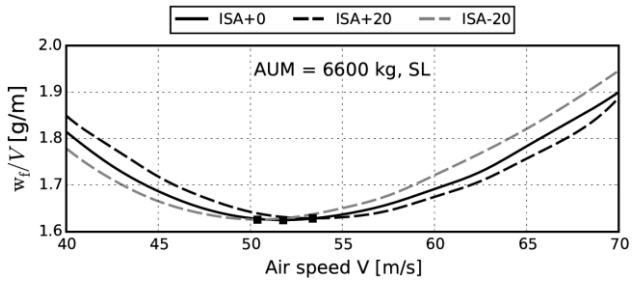

b)

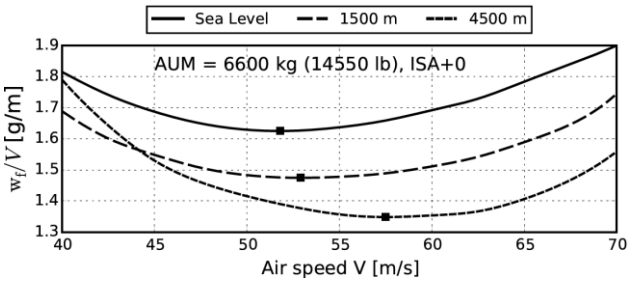

c)

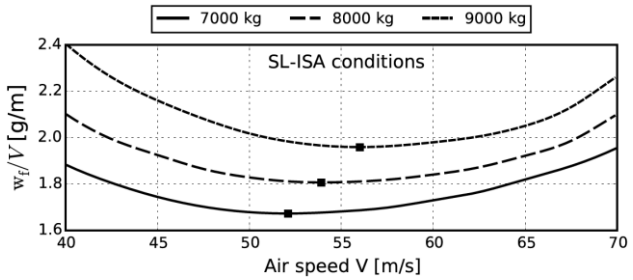

Figure 11 Airspeed for maximum range at different: (a) ambient temperature, (b) flight altitude, (c) helicopter AUM

a)

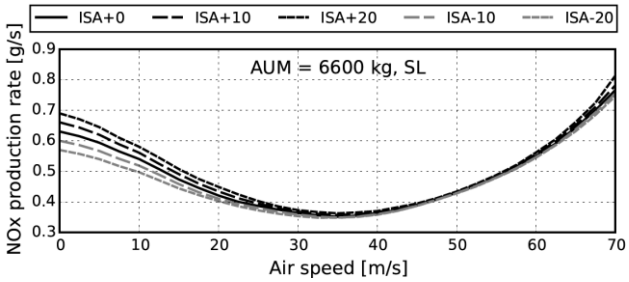

b)

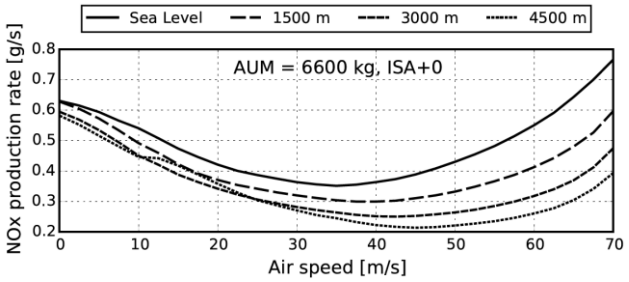

c)

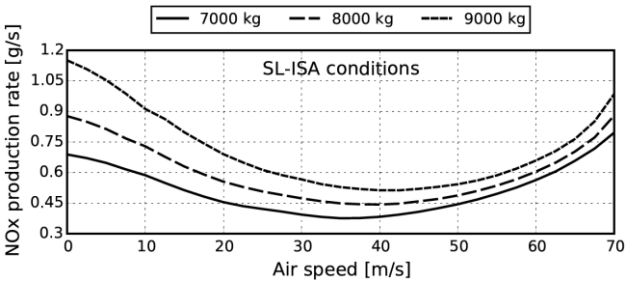

Figure 12 Powerplant NO_x formation rate in forward flight at different: (a) ambient temperature, (b) flight altitude, (c) helicopter AUM

a)

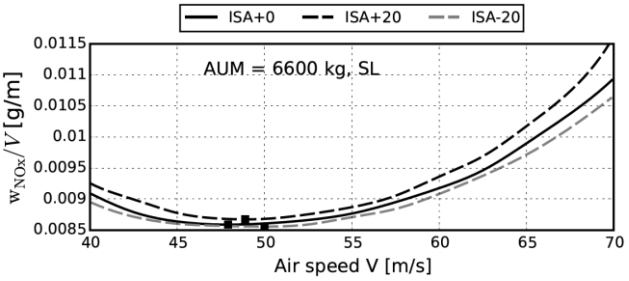

b)

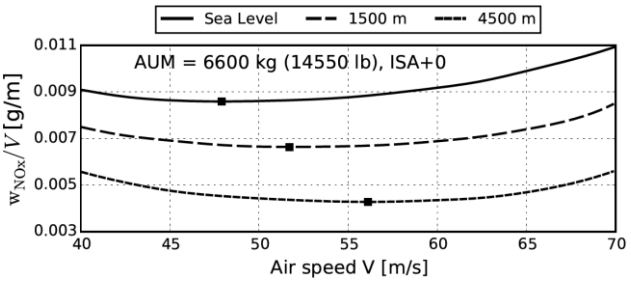

c)

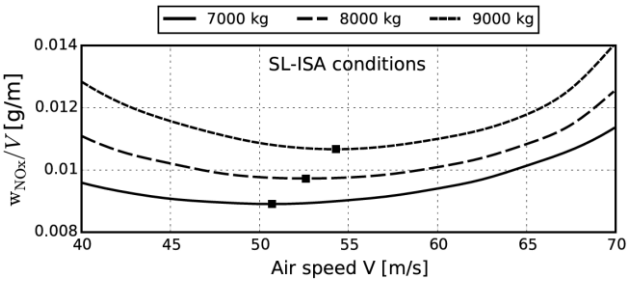

Figure 13 Airspeed for minimum NO_x formation at different: (a) ambient temperature, (b) flight altitude, (c) helicopter AUM

a)

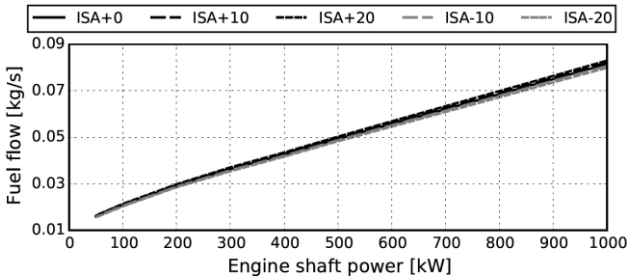

b)

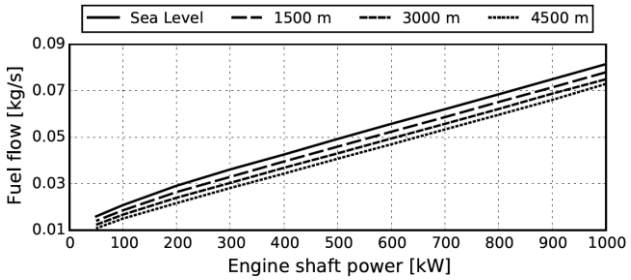

c)

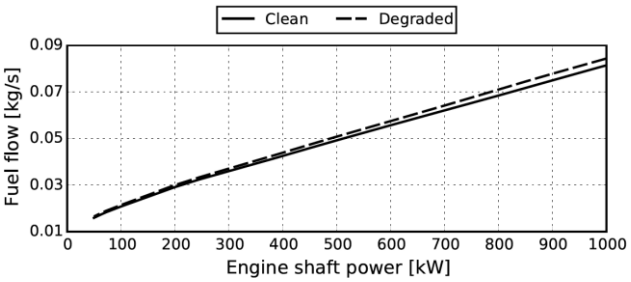

Figure 14 Fuel flow vs. shaft power at different: (a) ambient temperature, (b) flight altitude, (c) compressor degradation ($\Delta\eta$ =-2.5%, $\Delta\Gamma$= -5%)

a)

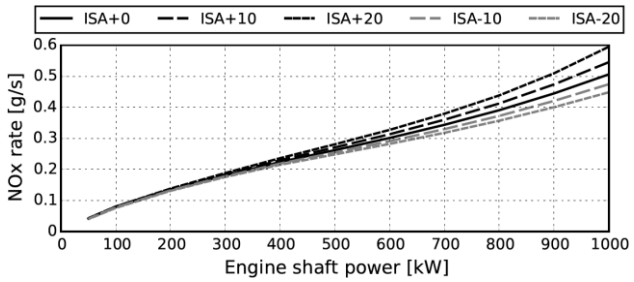

b)

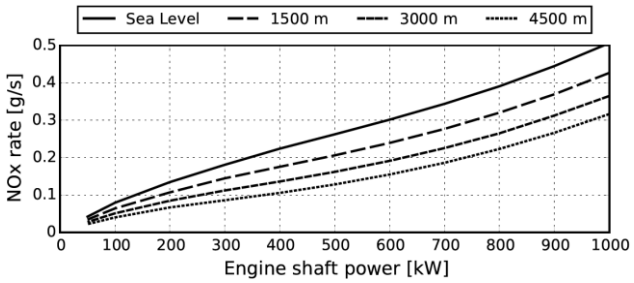

c)

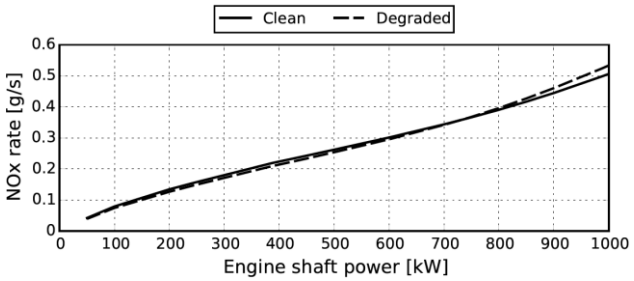

Figure 15 NO_x production rate vs. shaft power at different: (a) ambient temperature, (b) flight altitude, (c) compressor degradation ($\Delta\eta$ =-2.5%, $\Delta\Gamma$= -5%)

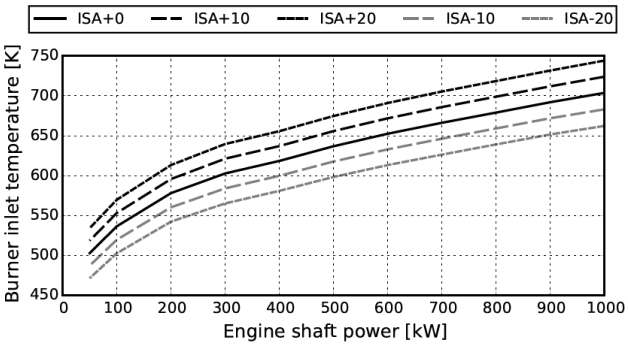

Figure 16 Combustor inlet temperature vs. shaft power at different ambient temperature

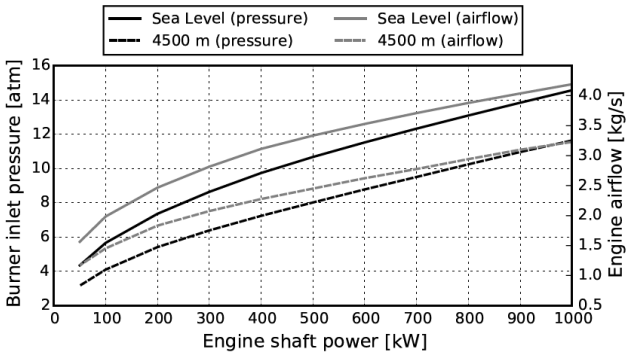

Figure 17 Combustor inlet pressure and airflow vs. shaft power at different altitude

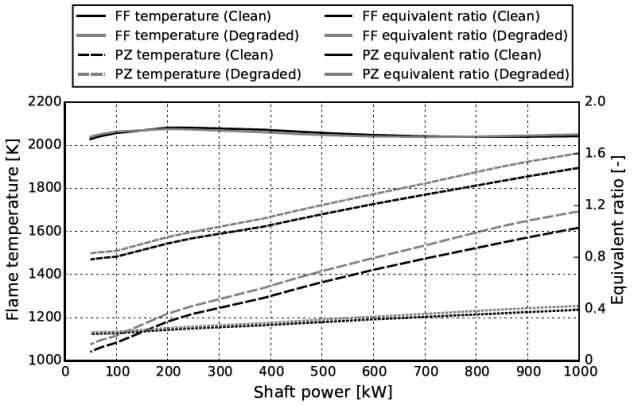

Figure 18 Combustor FF and PZ flame temperature and equivalent ratio vs. shaft power: effect of compressor degradation ($\Delta\eta$ =-2.5%, $\Delta\Gamma$= -5%)

a)

b)

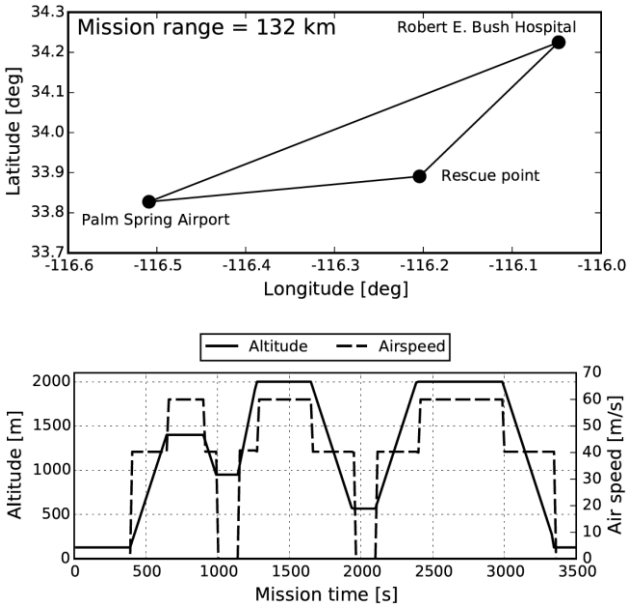

Figure 19 EMS mission definition: (a) geographical trajectory, (b) altitude and airspeed vs. time

a)

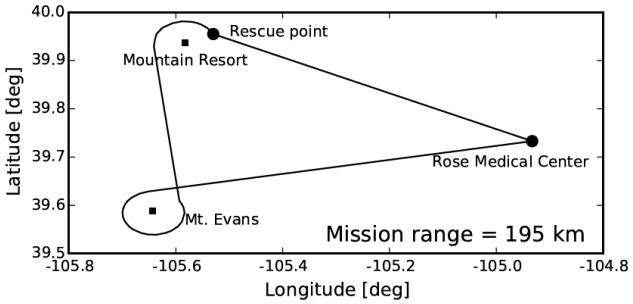

b)

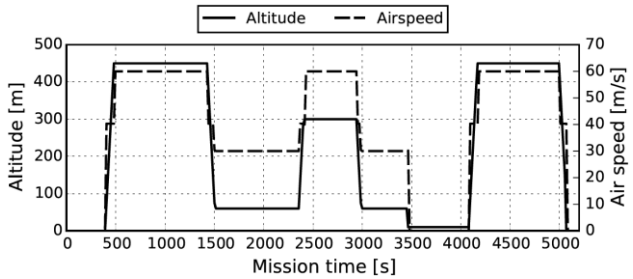

c)

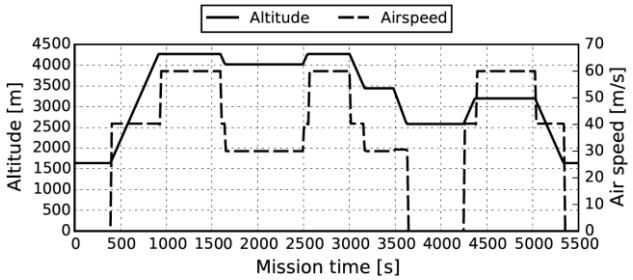

Figure 20 SAR mission definition: (a) geographical trajectory, (b) altitude and airspeed vs. time (SL scenario), (c) altitude and airspeed vs. time ('High & Cold' scenario)

a)

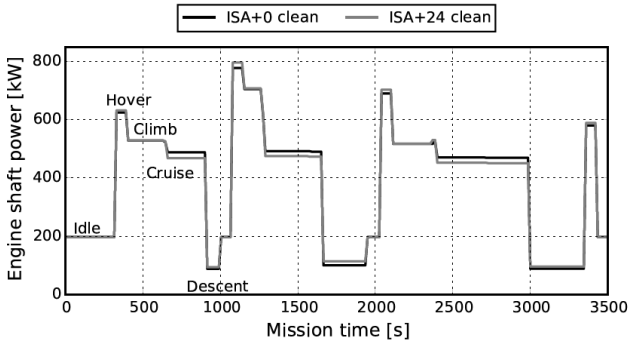

b)

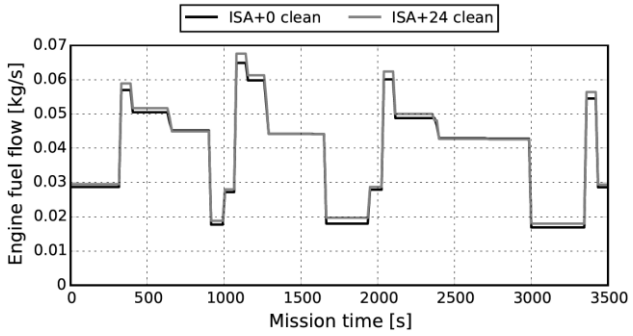

c)

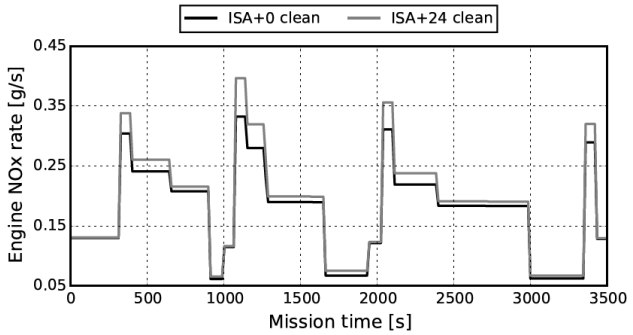

Figure 21 Effect of temperature on EMS mission: (a) engine power, (b) fuel flow, (c) NO_x rate

a)

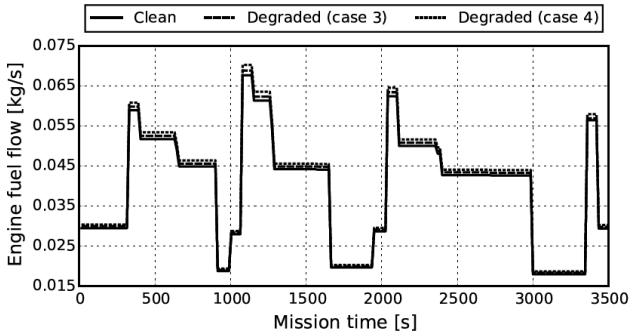

b)

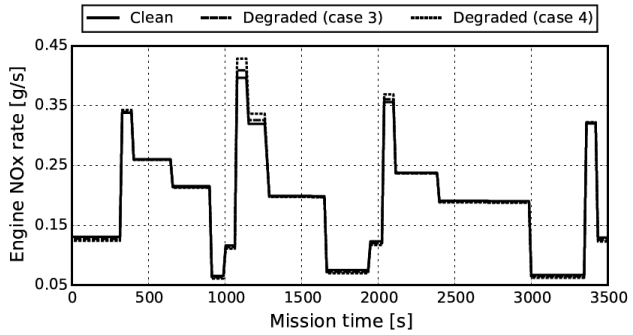

Figure 22 Effect of degradation on EMS mission: (a) fuel flow, (b) NO_x rate

a)

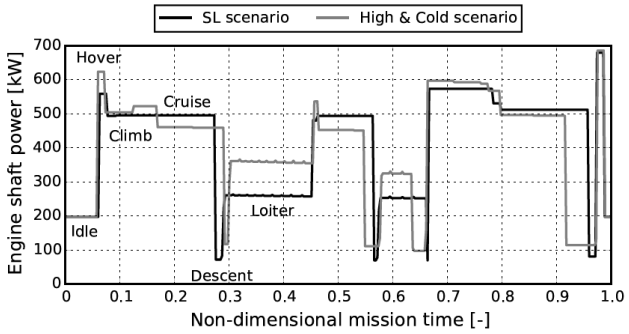

b)

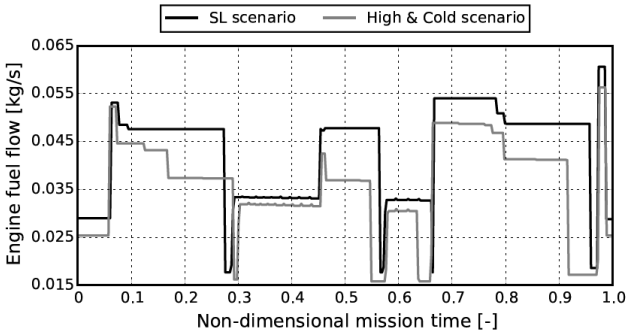

c)

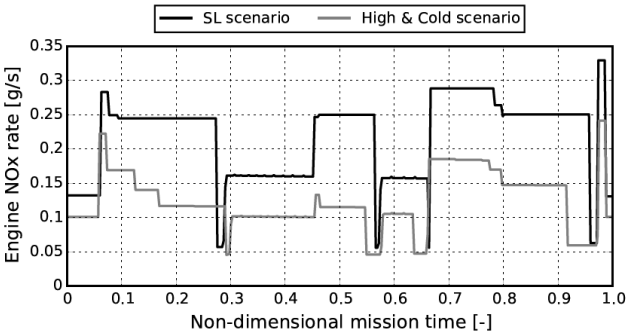

Figure 23 Effect of altitude and temperature on SAR mission: (a) engine power, (b) fuel flow, (c) NO_x rate

Cranfield University

CERES Research Repository **https://dspace.lib.cranfield.ac.uk/**

School of Aerospace, Transport and Manufacturing (SATM) Staff publications (SATM)

Impact of adverse environmental conditions on rotorcraft operational performance and pollutant emissions

Ortiz Carretero, Jesus

2017-08-23

Attribution 4.0 International

Jesus Ortiz-Carretero, Alejandro Castillo Pardo, Ioannis Goulos and Vassilios Pachidis. Impact of adverse environmental conditions on rotorcraft operational performance and pollutant emissions. Journal of Engineering for Gas Turbines and Power, Volume 140, Issue 2, Article number 021201, October 2017. Paper No: GTP-17-1313

https://doi.org/10.1115/1.4037751

Downloaded from CERES Research Repository, Cranfield University